Tailor-Made Core-Shell CaO/TiO2-Al2O3 Architecture as a High-Capacity and Long-Life CO2 Sorbent

Article *in* Environmental Science & Technology · June 2015

DOI: 10.1021/acs.est.5b01415 · Source: PubMed

Zuwei Xu
Huazhong University of Science and Technol…

Cong Luo
Huazhong University of Science and Technol…

Haibo Zhao
Huazhong University of Science and Technol…

Environmental Science & Technology

Article

pubs.acs.org/est

Tailor-Made Core−Shell $CaO/TiO_2-Al_2O_3$ Architecture as a High-Capacity and Long-Life CO_2 Sorbent

Weiwei Peng,[†,‡,§] Zuwei Xu,[†,§] Cong Luo,[†] and Haibo Zhao*[,†,‡]

[†]State Key Laboratory of Coal Combustion, Huazhong University of Science and Technology, 1037 Luoyu Road, Wuhan 430074, China

[‡]China-EU Institute for Clean and Renewable Energy, Huazhong University of Science and Technology, 1037 Luoyu Road, Wuhan 430074, China

Supporting Information

ABSTRACT: CaO-based sorbents are widely used for CO_2 capture, steam methane reforming, and gasification enhancement, but the sorbents suffer from rapid deactivation during successive carbonation/calcination cycles. This research proposes a novel self-assembly template synthesis (SATS) method to prepare a hierarchical structure CaO-based sorbent, Ca-rich, Al_2O_3-supported, and TiO_2-stabilized in a core−shell microarchitecture ($CaO/TiO_2-Al_2O_3$). The cyclic CO_2 capture performance of $CaO/TiO_2-Al_2O_3$ is compared with those of pure CaO and CaO/Al_2O_3. $CaO/TiO_2-Al_2O_3$ sorbent achieved superior and durable CO_2 capture capacity of 0.52 g CO_2/g sorbent after 20 cycles under the mild calcination condition and retained a high-capacity and long-life performance of 0.44 g CO_2/g sorbent after 104 cycles under the severe calcination condition, much higher than those of CaO and CaO/Al_2O_3. The microstructure characterization of $CaO/TiO_2-Al_2O_3$ confirmed that the core−shell structure of composite support effectively inhibited the reaction between active component (CaO particles) and main support (Al_2O_3 particles) by TiO_2 addition, which contributed to its properties of high reactivity, thermal stability, mechanical strength, and resistance to agglomeration and sintering.

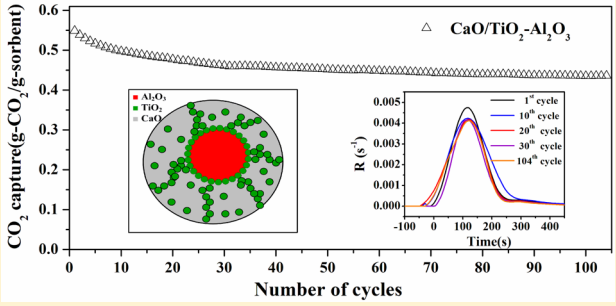

1. INTRODUCTION

CO_2 emission into the atmosphere is one of main factors that brings about global warming and environment change, which has been a public concern in recent years.[1−3] Thirty-three percent of industrial CO_2 emission comes from high-temperature flue gas of fossil fuel combustion, and the need to mitigate CO_2 emissions by developing CO_2 capture and storage (CCS) technology is now widely accepted.[4,5] CaO-based CO_2 sorbent has received a great deal of attention due to its low material cost, abundant source, and high CO_2 capture capacity (1 g of CaO can absorb 0.786 g of CO_2 in theory). CaO-based sorbents can effectively remove CO_2 from combustion or gasification gases at high temperature, allowing it to be regenerated in calcination process as a pure CO_2 stream suitable for use or, more likely, for storage.[6,7] Normally, calcium looping (Ca-L), which is based on the reversible carbonation/calcination reaction of CaO, becomes one of the most promising technologies for CCS[8−11] and for advanced gasification or reforming.[12,13] However, the major challenge in developing Ca-L technology is the problem of loss-in-capacity, i.e. the loss in initial capture capacity in successive carbonation/calcination cycles.[14−16] For the carbonation reaction, it has been well reported that a rapid and chemically controlled reaction period is followed by a slow diffusion period.[17−19] It has been reported that the transition between the fast and slow reaction periods occurs quite suddenly at a given level of conversion, which decreases rapidly with increasing carbonation/calcination cycles.[12,20,21] This change of the reaction rate is attributed to the formation of a product layer of about 50 nm thick.[22,23] In addition, the molar volume of $CaCO_3$ formed is much larger than that of CaO, which leads to pore blocking and an increase in diffusion resistance of CO_2 through the carbonation product layer.[6,24] Also, a structural and morphological change of sorbent occurs during cyclic reaction due to low sintering temperature (approximately 529 °C) of $CaCO_3$. Therefore, it is significant to alleviate the rapid decay of CaO-based sorbents and obtain the CaO-based sorbent possessing properties of high reactivity, thermal stability, mechanical strength, and resistance to agglomeration and sintering.

Great efforts have been made to overcome the loss-in-capacity problem.[24−26] Synthesizing CaO-based composite materials is regarded as one of the most efficient methods.[27−34] Among various supports of the active component CaO, Al_2O_3 has received considerable attention for its high melting point

Received: March 20, 2015
Revised: May 21, 2015
Accepted: June 5, 2015
Published: June 5, 2015

DOI: 10.1021/acs.est.5b01415
Environ. Sci. Technol. 2015, 49, 8237−8245

and high mechanical strength, which contribute to increasing temperature resistance and improving durability of CaO-based sorbents.[32,35−38] Manovic et al.[39] found that La Blanca (LB) limestone, which did not originally contain significant Al, showed increased reactivity after Al_2O_3 doping, thus the absence of Al in the original LB sample was suggested as a likely cause for its poor performance. Martavaltzi et al.[40] reported that a $CaO/Ca_{12}Al_{14}O_{33}$ sorbent obtained 6 mol/kg CO_2 fixed amount after 45 successive cycles under cyclic conditions of carbonation at 690 °C for 30 min in 15 vol % CO_2 and calcination at 850 °C in pure N_2 for 10 min. As mentioned above, it was concluded that CaO/Al_2O_3-based sorbents significantly improved CO_2 capture and cyclic reaction stability over multiple carbonation/calcination cycles. However, multiple types of calcium aluminate were formed during the preparation process or cyclic test of CaO/Al_2O_3-based sorbents at high temperatures by interaction between CaO and Al_2O_3, resulting in the partial loss of CaO. In addition, the reaction product was hard to control due to complexity of the chemical reaction caused by variations in precursor, preparation method, and cyclic condition. Florin et al.[41] proposed a precipitation method to prepare $CaO/Ca_{12}Al_{14}O_{33}$ using inexpensive and commercially available raw materials. They obtained 75% conversion during the first cycle at 650 °C for 10 min carbonation under 15 vol % CO_2, but experienced 50% deactivation after 30 cycles (calcination at 900 °C, 15 vol % CO_2, 5 min). Li et al.[42] showed that $CaO/Ca_{12}Al_{14}O_{33}$, prepared by wet mixing method, attained 41 wt % CO_2 capture capacity after 50 carbonation/calcination cycles under mild calcination conditions (850 °C, 100% N_2). However, the capture capacity of sorbent decreased from 52 wt % in the first cycle to about 22 wt % in the 56th cycle when severe calcination conditions (980 °C, 100% CO_2) were used. The chemical reactions between CaO and Al_2O_3,[42] which might happen at high temperatures, are shown as follows:

$$7Al_2O_3 + 12CaO \rightarrow Ca_{12}Al_{14}O_{33} \quad (R1)$$

$$5Al_2O_3 + Ca_{12}Al_{14}O_{33} \rightarrow 12CaAl_2O_4 \quad (R2)$$

$$Al_2O_3 + CaO \rightarrow CaAl_2O_4 \quad (R3)$$

$$7CaAl_2O_4 + 5CaO \rightarrow Ca_{12}Al_{14}O_{33} \quad (R4)$$

$$Ca_{12}Al_{14}O_{33} + 9CaO \rightarrow 7Ca_3Al_2O_6 \quad (R5)$$

In this work, a self-assembly template synthesis (SATS) method is proposed to synthesize a hierarchical structure CaO-based sorbent, Ca-rich, Al_2O_3-supported, and TiO_2-stabilized in a core−shell microarchitecture ($CaO/TiO_2-Al_2O_3$). $CaO/TiO_2-Al_2O_3$ sorbent is based on the self-assembly between TiO_2 nanoparticles (nano-TiO_2) and Al_2O_3 microparticles (micron-Al_2O_3), where nano-TiO_2 particles are coated on the surface of micron-Al_2O_3 particles to inhibit the interaction of active phase CaO with the main support Al_2O_3. In addition, cyclic carbonation/calcination tests under different conditions and microstructure characterization of $CaO/TiO_2-Al_2O_3$ are compared with that of CaO and CaO/Al_2O_3 to prove the superiority of the SATS-derived CO_2 sorbent.

2. EXPERIMENTAL SECTION

2.1. Materials. In this study, calcium acetate monohydrate power (Sinopharm Chemical Reagent Co. Ltd., Shanghai, China) was used as calcium precursor. Commercial Al_2O_3 powder (Sinopharm Chemical Reagent Co. Ltd., Shanghai, China) with larger than 200 meshes (i.e., particle size <75 μm) was selected as the main component of the support. Flame-synthesized TiO_2 nanoparticles were deposited on the surface of Al_2O_3 by electrostatic self-assembly in precursors to modify and stabilize the support. The flame-synthesized TiO_2 nanoparticle was manufactured by a gas flame synthesis facility in which a four-concentric-tube burner was fed with $TiCl_4$ and N_2, CH_4, O_2, and N_2, from the center to the outside.[43] The detailed operating conditions and experimental data about the flame synthesis are available in the Supporting Information (SI).

2.2. Preparation of Sorbents. *2.2.1. Sample A: Preparation of Pure CaO by Calcination Method.* A calculated amount of calcium acetate monohydrate was directly calcined in a muffle furnace at 950 °C for 2 h; the derived product was sample A.

2.2.2. Sample B: Preparation of CaO/Al_2O_3 (80 wt % CaO:20 wt % Al_2O_3) by Wet Impregnation Method. The preparation procedures were as follows. Step 1: A calculated amount of Al_2O_3 powder was put into an electric-heated thermostatic water bath to adequately mix with 400 mL of distilled water at 80 °C for 30 min. Step 2: Calcium acetate monohydrate was added at the mass ratio of CaO to Al_2O_3 of 4:1 with stirring for 30 min. Step 3: The wet precursor was dried in an electrically heated drying oven at 80 °C for 24 h, and finally was calcined at 950 °C in the muffle furnace for 2 h.

2.2.3. Sample C: Preparation of $CaO/TiO_2-Al_2O_3$ (80 wt % CaO:5 wt % TiO_2:15 wt % Al_2O_3) by Self-Assembly Template Synthesis Method. The first step was the same as that of sample B. Step 2: A calculated amount of nano-TiO_2 (the mass ratio of Al_2O_3 to TiO_2 of 3:1 was used to ensure complete coverage of core-structured micron-Al_2O_3 by shell-structured nano-TiO_2) was added into the electrically heated thermostatic water bath, and the pH value of the suspension was adjusted to 6 by titrating dilute acetic acid or ammonia solution with consecutive stirring for 30 min. Step 3: Calcium acetate monohydrate was added at the mass ratio of CaO to Al_2O_3 of 16:3 under the conditions of full stirring. Step 4: The precursor was then dried at 80 °C for 24 h, resulting in fluffy and snowflake-like materials (shown in SI Figure S4). The dried precursor was subsequently calcined at 950 °C in the muffle furnace for 2 h.

All of the as-prepared samples were annealing cooled, ground, and screened. Finally, samples with a particle size range of 75−150 μm were selected.

2.3. Cyclic Carbonation/Calcination Tests. The cyclic performance of three samples was tested under mild and severe calcination conditions. Twelve mg of sample was placed in a zirconia copple of a thermogravimetric analyzer (Beijing Optical Instrument Factory, WCT-1D) and was heated to 700 °C at a rate of 15 °C/min under an N_2 flow of 60 mL/min. After complete precalcination at 700 °C for 30 min, 20 carbonation/calcination cyclic tests were conducted continuously under conditions of alternating atmospheres (10 vol % CO_2 (balanced with N_2) for carbonation process and pure N_2 for calcination process) and constant temperature of 700 °C, and each process lasted 20 min. CO_2 capture capacity was calculated on the basis of mass change, assuming this occurred only due to formation/decomposition of $CaCO_3$.

In consideration of high calcination temperatures (850−1000 °C) and high CO_2 concentrations (> vol 90%) in practical industrial processes, the cyclic test under the severe calcination condition was investigated by using a simultaneous thermal analyzer (Netzsch, STA499F3). Approximately 35 mg of each

DOI: 10.1021/acs.est.5b01415
Environ. Sci. Technol. 2015, 49, 8237−8245

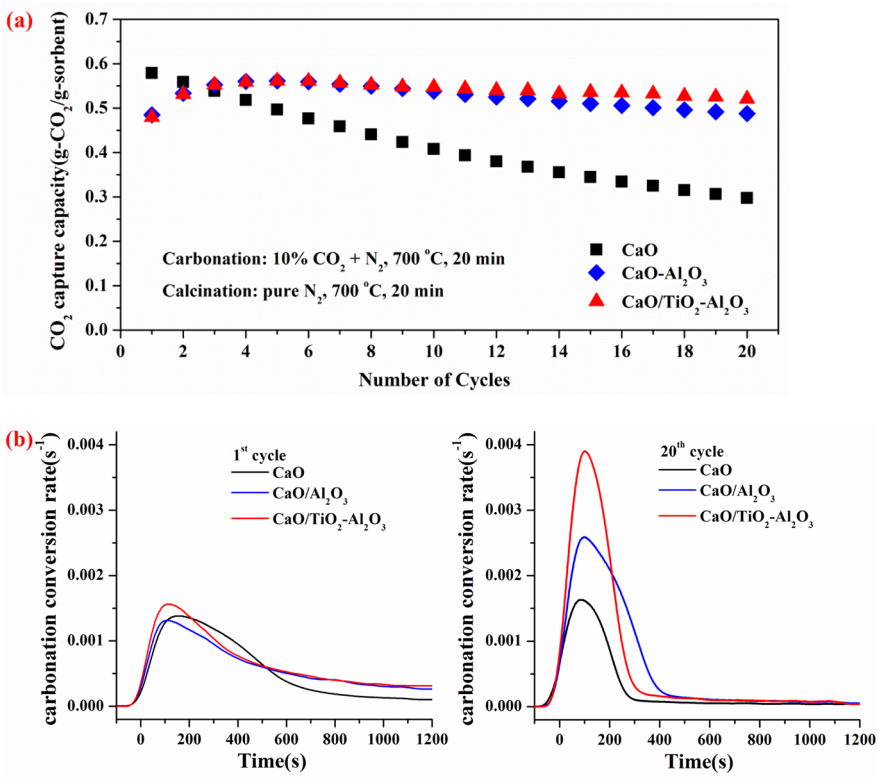

Figure 1. CO_2 capture performance of CaO, CaO/Al_2O_3, and $CaO/TiO_2-Al_2O_3$ under mild calcination condition: (a) evolution of CO_2 capture capacity during 20 cycles, (b) evolution of carbonation reaction rate at first and 20th cycle. Carbonated at 700 °C in 10 vol % CO_2 for 20 min and calcined at 700 °C in pure N_2 for 20 min.

sample was heated to 900 °C at a rate of 20 °C/min under an N_2 flow of 100 mL/min, and lasted for 30 min for initial complete calcination. The temperature was then reduced to 700 °C for carbonation process with a 10 vol % CO_2 (balanced with N_2) flow of 100 mL/min for 20 min. The temperature was then increased to 900 °C for calcination process with pure CO_2 for 5 min. Thirty carbonation/calcination cycles were conducted for CaO and CaO/Al_2O_3, while 104 cycles were conducted for $CaO/TiO_2-Al_2O_3$.

2.4. Characterization Techniques. Fresh and used sorbents (exposed to the severe calcination condition of 900 °C in pure CO_2) were used for characterization techniques. The crystalline phase of sorbents was determined by X-ray diffraction (XRD, X'Pert Pro) using Cu Kα radiation (λ = 0.1542 nm) in a 2θ range of 10−90° with an accelerating voltage of 40 kV and tube current of 40 mA. The microstructure was investigated by field scanning electron microscope (FSEM, FEI Sirion200) with 10 kV of accelerating voltage and by transmission electron microscopy (TEM, Tecnai Gw F30, FEI Inc.) with 200 kV of accelerating voltage. The FSEM was equipped with an X-ray energy dispersive spectrometer (X-ray EDS), which enabled the analysis of elemental composition and dispersion determination. The pore structure parameters were measured by a Micrometrics ASAP 2020 apparatus, and the surface area and pore volume were calculated from the Brunauer−Emmet−Teller (BET) equations and the Barrett−Joyner−Halenda (BJH) method, respectively. A digital dynamometer (Shimpo FGJ-5) was used to measure the crushing strength of CaO-based sorbents.

3. RESULTS AND DISCUSSION

3.1. Evolution of CO_2 Capture Performance under Mild and Severe Calcination Conditions. Twenty consecutive cyclic tests for three types of sorbents were conducted at the mild calcination condition with 700 °C in pure N_2 (shown in Figure 1). CaO sorbent (sample A), which was used as a comparative sorbent without adding any support, exhibited maximum initial CO_2 capture capacity of 0.58 g CO_2/g sorbent (g/g for logogram in following descriptions, all of calculation formulas in this study are presented in the SI), compared with 0.49 and 0.48 g/g for CaO/Al_2O_3 (sample B) and $CaO/TiO_2-Al_2O_3$ (sample C), respectively. However, a serious loss-in-capacity phenomenon of CaO sorbent happened after 20 cycles, which was consistent with previous research.[44,45] In contrast, the CO_2 capture capacity of CaO/Al_2O_3 and $CaO/TiO_2-Al_2O_3$ maintained 0.49 and 0.52 g/g, respectively, after 20 cycles, presenting superior performance in terms of both capture capacity and stability. It was noted that the CO_2 capture capacity of CaO/Al_2O_3 and $CaO/TiO_2-Al_2O_3$ increased from 0.48 to 0.56 g/g in the first 4 cycles. This increasing CO_2 capture behavior in the initial few cycles is called self-reactivation phenomenon, and has also been reported in other literature.[46,47] Moreover, $CaO/TiO_2-Al_2O_3$ showed better cyclic stability than CaO/Al_2O_3 from the 11th cycle, and the advantage of $CaO/TiO_2-Al_2O_3$ was also verified by carbonation reaction rate (shown in Figure 1b), which was especially reflected in an evident difference of reactivity at the 20th carbonation process. The considerable CO_2 capture performance of CaO/Al_2O_3 and $CaO/TiO_2-Al_2O_3$ could be attributed to the high mechanical strength, durability, and sintering resistance of Al-based materials.[10,35,47]

DOI: 10.1021/acs.est.5b01415
Environ. Sci. Technol. 2015, 49, 8237−8245

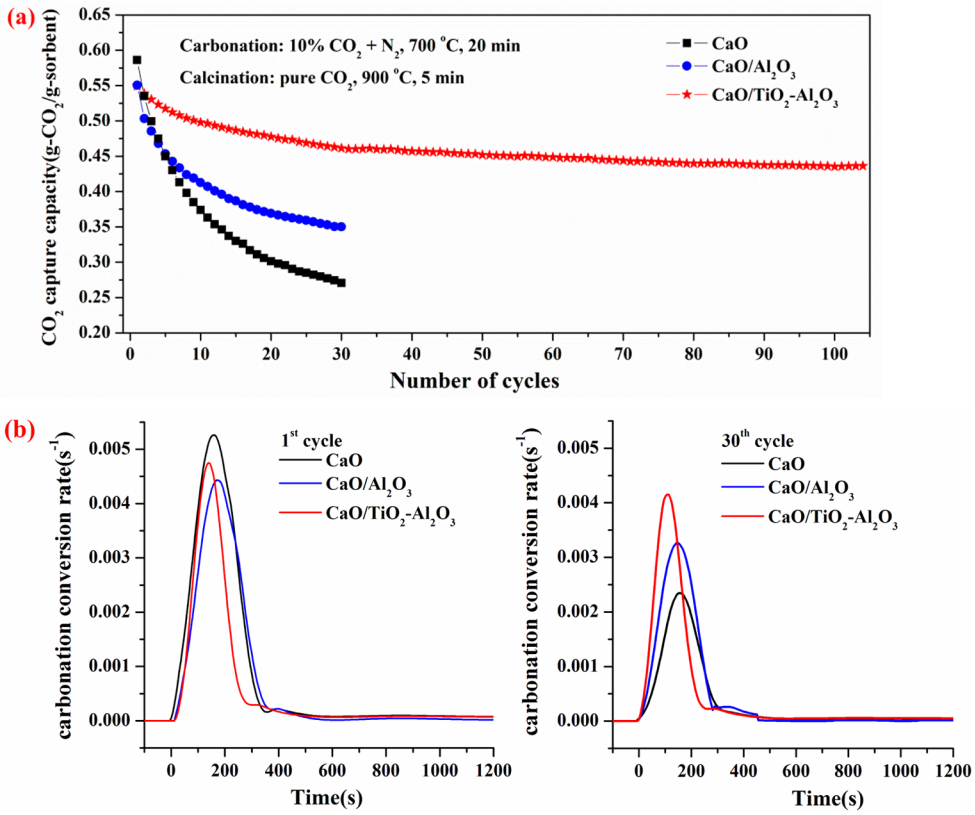

Figure 2. CO_2 capture performance of CaO, CaO/Al_2O_3, and $CaO/TiO_2-Al_2O_3$ under severe calcination condition: (a) evolution of CO_2 capture capacity during multiple cycles, (b) evolution of carbonation reaction rate at first and 30th cycle. Carbonated at 700 °C in 10 vol % CO_2 for 20 min and calcined at 900 °C in pure CO_2 for 5 min.

The CO_2 capture performance of three sorbents under the severe calcination condition (900 °C in pure CO_2) is presented in Figure 2a. Three sorbents exhibited considerable and approximate CO_2 capture capacity at the first cycle; however, a decrease in CO_2 capture capacity with an increasing number of cycles occurred for all sorbents. More specifically, CO_2 capture capacity of CaO/Al_2O_3 decreased to 0.35 g/g after 30 cycles, which was much different from that shown Figure 1. One explanation for this difference was that the active CaO reacted with Al-based material at the severe calcination condition, causing the significant reduction in CO_2 capture capacity. Nonetheless, the CO_2 capture capacity of CaO/Al_2O_3 still slowly exceeded that of pure CaO at the fifth cycle and this superiority was kept in the remaining cycles.

As for $CaO/TiO_2-Al_2O_3$, it maintained a capture capacity of approximately 0.46 g/g after 30 cycles, which was 31.8% and 70.6% higher than those of CaO/Al_2O_3 and CaO, respectively. Even after 104 cycles, it still attained superior capture capacity of 0.44 g/g, retaining 79.4% of the initial CO_2 absorbing amount. Compared with carbonation reaction rate at the first and 30th cycles (shown in Figure 2b), it was demonstrated that CaO lost its fast reaction rate with increasing of cycles. In contrast, the outstanding reactivity of $CaO/TiO_2-Al_2O_3$ was retained during 30 cycles. The fast carbonation reaction rate was dominated by a high content of crystalline CaO.

It is concluded that the CO_2 capture capacity of CaO/Al_2O_3 in the severe condition did not perform as well as that in the mild condition; however, the SATS-derived $CaO/TiO_2-Al_2O_3$ has superior CO_2 capture capacity and cyclic reaction stability over multiple cycles in either the mild or severe conditions.

3.2. Physicochemical Characterizations of CaO-Based Sorbents. The BET−BJH results shown in Figure 3a demonstrate that the specific surface area and specific pore volume of sorbents reduced with the increase of cycle number, especially within the first 10 cycles, which was in accordance with the change trend of reactivity decay shown in Figure 2, indicating CaO-based sorbents achieved a maximum falloff limit after 10 cycles. During 30 cyclic tests at 900 °C, the decay ratios in specific surface area of CaO and CaO/Al_2O_3 were as high as about 97% and 82%, respectively. For $CaO/TiO_2-Al_2O_3$ specific surface area was changed from 24.85 to 12.36 m^2/g during 30 cycles, corresponding to a decay ratio of 50.2%. The change trend of specific pore volume was in accordance with that of surface area. Higher specific surface area and specific pore volume of $CaO/TiO_2-Al_2O_3$ result directly in good cyclic capacity, and the fact that $CaO/TiO_2-Al_2O_3$ maintained its high surface area and pore volume further proved that $CaO/TiO_2-Al_2O_3$ had excellent sintering resistance. Pore size distribution shown in Figure 3b exhibited a loss in small pores for both CaO and $CaO/TiO_2-Al_2O_3$ after 30 cycles, which was attributed to agglomeration and sintering among different particles under high calcination temperature of 900 °C. Nevertheless, the SATS-derived $CaO/TiO_2-Al_2O_3$ demonstrated more abundant mesopores and wider pore size distribution compared with pure CaO sorbent. It was noted that the surface of pores 30−100 nm in diameter for the $CaO/TiO_2-Al_2O_3$ sorbent, which was important for CO_2 adsorption, was smaller than that for CaO. However, the surface of pores 30−100 in nm diameter for the used $CaO/TiO_2-Al_2O_3$ sorbent after 30 cycles is much larger than that of used CaO. This may be attributed to competition between positive "self-

DOI: 10.1021/acs.est.5b01415
Environ. Sci. Technol. 2015, 49, 8237−8245

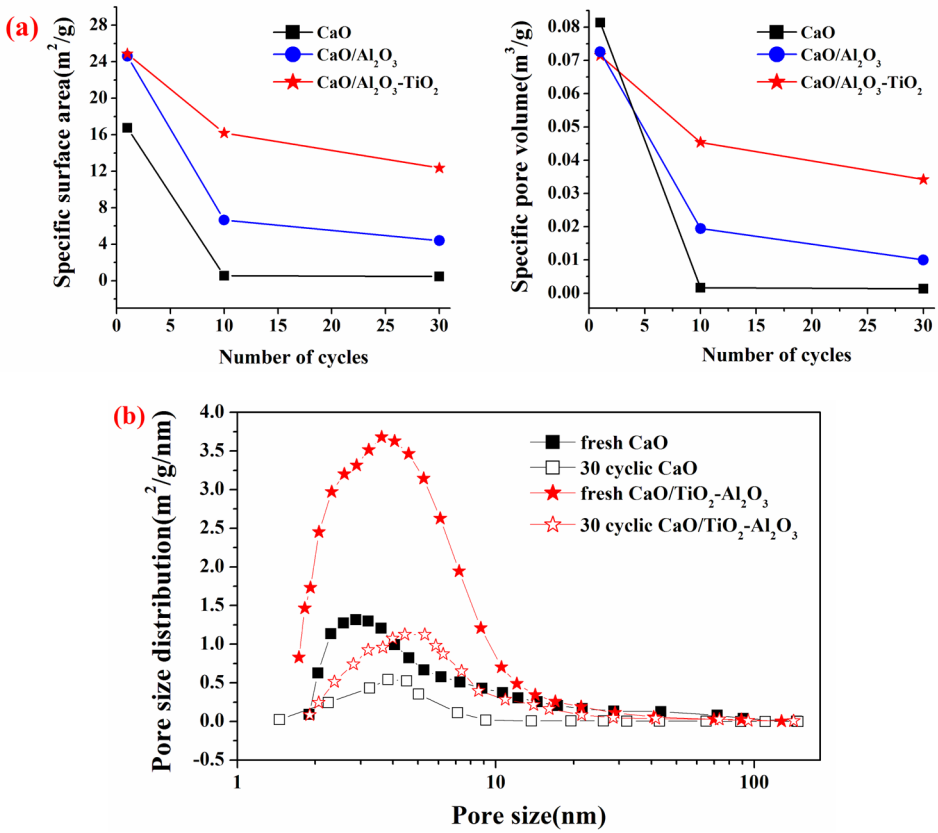

Figure 3. (a) Specific surface area and specific pore volume results for fresh and used CaO, CaO/Al_2O_3, and $CaO/TiO_2-Al_2O_3$. (b) Pore size distribution results for fresh and used CaO and $CaO/TiO_2-Al_2O_3$. Tests of used CaO and $CaO/TiO_2-Al_2O_3$ were conducted in severe calcination condition of 900 °C in pure CO_2.

activation" function and negative sintering effect of $CaO/TiO_2-Al_2O_3$ sorbent, which is described in detail in the SI.

From Figure 4, fresh sorbents had developed porous structure, which provided a larger surface area and was beneficial to carbonation reaction. It was found that a significant change of the samples in porosity and morphology appeared after 30 cycles. Sample A suffered from the most serious sintering: CaO grains developed a dense layer structure, and pore blockage in pore channels, aggregation of crystals, serious sintering texture, and small cracks were clearly observed (shown in Figure 4d, g). As for calcined CaO/Al_2O_3, its particle size was smaller than that of CaO and interpenetration still existed among different pores, meaning the sintering degree of CaO/Al_2O_3 was less serious than that of CaO. In contrast, the microstructure of $CaO/TiO_2-Al_2O_3$ was more porous and crystal aggregation was not too critical, which contributed to prominent CO_2 capture capacity in multiple cycles.[48,49]

3.3. Discussion of the Novel SATS-Derived $CaO/TiO_2-Al_2O_3$ Sorbent. From the above experimental results, we found that $CaO/TiO_2-Al_2O_3$ possessed better physicochemical performance, and the reason for its outstanding performance deserved further investigation and analysis. One possible explanation is its unique preparation method, i.e. the self-assembly template synthesis (SATS) method, which is based on nano/micron-particle coating technology, allowing a customized hierarchical structure (typically, core−shell composite) derived from the self-assembly of different particles. The hydration between inorganic oxide particles and water can produce hydroxyl groups, and the surface of particles is charged due to hydroxyl dissociation.[50] The particle surface potential (zeta potential) can be regulated by the pH value, whereby unlike particles (here nano-TiO_2 and micron-Al_2O_3) can be charged with opposite potential.[51] SI Figure S8 shows the zeta potential of micron-Al_2O_3 and nano-TiO_2 as a function of pH of the aqueous dispersions as measured by a microelectrophoresis apparatus (Powereach JS94H, Shanghai Zhongchen Digital Technical Apparatus Co., Ltd., China). When the pH value of the dispersion system was readjusted to 6 by adding dilute acetic acid or ammonia solution, the surface potential of micron-Al_2O_3 (isoelectric point of 9.0) was maximally differentiated from that of flame-synthesized nano-TiO_2 (isoelectric point of 3.4). Under this condition, spontaneous aggregation between micron-Al_2O_3 and nano-TiO_2 particles occurred due to van der Waals force and electrostatic attractive force. Thus, a complete coating of micron-Al_2O_3 was realized by a small amount of nano-TiO_2 in precursor solution. This core−shell structure was effectively helpful for the high performance of synthetic oxygen carrier in a previous study.[52] This way, the reaction between CaO and Al_2O_3 was prevented in the subsequent carbonation/calcination cycles. A schematic sketch of preparation process of SATS-derived $CaO/TiO_2-Al_2O_3$ is presented in Figure 5. This resultant sorbent with a high CaO content can withstand high temperature without serious sintering and agglomeration, thus keeping a high CO_2 capture capacity.

XRD patterns of CaO/Al_2O_3 and $CaO/TiO_2-Al_2O_3$ sorbents (shown in Figure 6) confirmed the superiority of SATS method. The chemical compositions of fresh $CaO/TiO_2-Al_2O_3$ were CaO, $Ca(OH)_2$, $CaTiO_3$, and Al_2O_3. After 30 cyclic tests, Al_2O_3 was still found in the sorbents, indicating

DOI: 10.1021/acs.est.5b01415
Environ. Sci. Technol. 2015, 49, 8237−8245

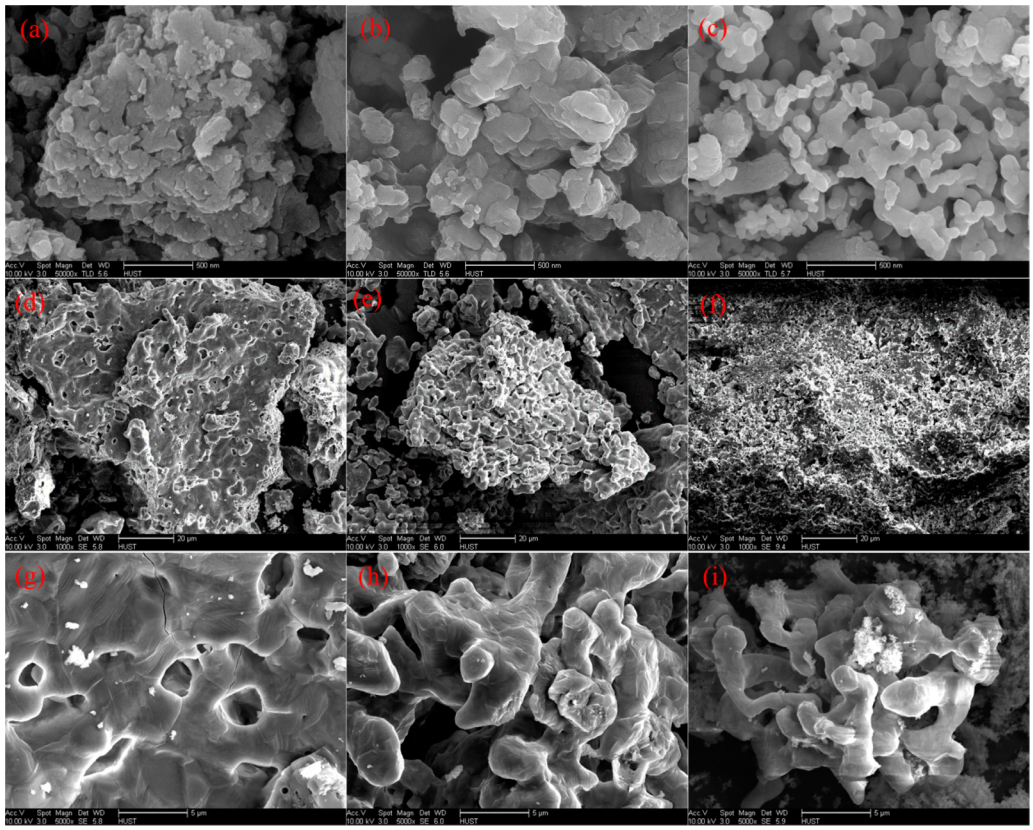

Figure 4. FSEM images of sorbents. Top row shows fresh sorbents with the magnifying power of 50 000 (a, b, and c). Middle row shows calcined sorbents after 30 cycles with the magnifying power of 1000 (d, e, and f). Bottom row shows calcined sorbents after 30 cycles with the magnifying power of 5000 (g, h, and i). Left column presents CaO (a, d, and g). Middle column presents CaO/Al_2O_3 (b, e, and h). Right column presents $CaO/TiO_2-Al_2O_3$ (c, f, and i).

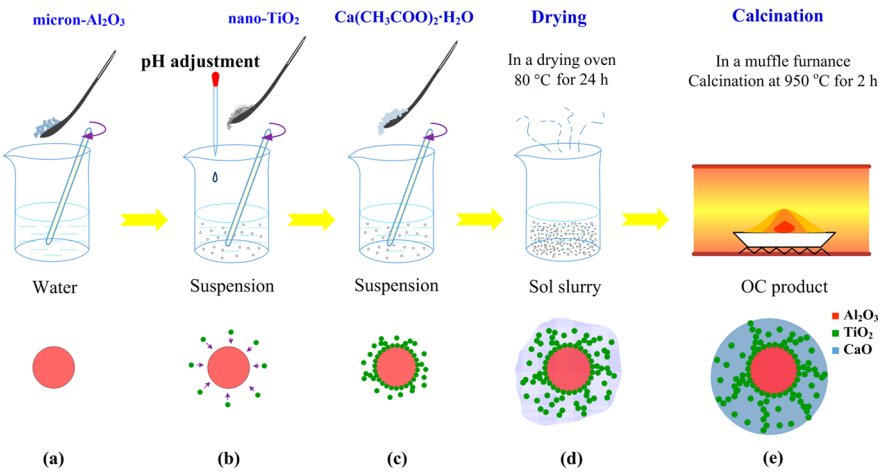

Figure 5. Schematic sketch of preparation process of SATS-derived $CaO/TiO_2-Al_2O_3$.

CaO did not react with Al_2O_3 during overall cyclic processes due to the inhibition effect of nano-TiO_2 shell. Meanwhile, the product $CaTiO_3$, which had high thermal stability and antisintering ability, was formed at high temperatures during the preparation process.[53] In comparison, $Ca_{12}Al_{14}O_{33}$ was formed in the fresh sample B due to the solid−solid reaction of CaO and Al_2O_3 upon the synthesis process, and the product $Ca_3Al_2O_6$ appeared because of deeper reaction between $Ca_{12}Al_{14}O_{33}$ and CaO (reactions R4 and R5 for reference). The existence of Ca−Al−O phase, either $Ca_{12}Al_{14}O_{33}$ or $Ca_3Al_2O_6$, illustrated active CaO suffered from continuous loss, which could explain the lower CO_2 capture capacity of CaO/Al_2O_3 in Figure 2.

Chemical composition changes of SATS-derived sorbent during cyclic reactions agreed with the proposed construction of CaO particles modified by core−shell structured $TiO_2-Al_2O_3$ composite support. Next, microstructure of TiO_2/Al_2O_3 skeleton (observed by TEM) and elemental dispersion determination of $CaO/TiO_2-Al_2O_3$ (observed by FSEM−EDS) were used to verify existence of the core−shell structure. The TEM image of $TiO_2-Al_2O_3$ skeleton (shown in Figure 7), which was obtained by dissolving fresh $CaO/TiO_2-Al_2O_3$ with

DOI: 10.1021/acs.est.5b01415
Environ. Sci. Technol. 2015, 49, 8237−8245

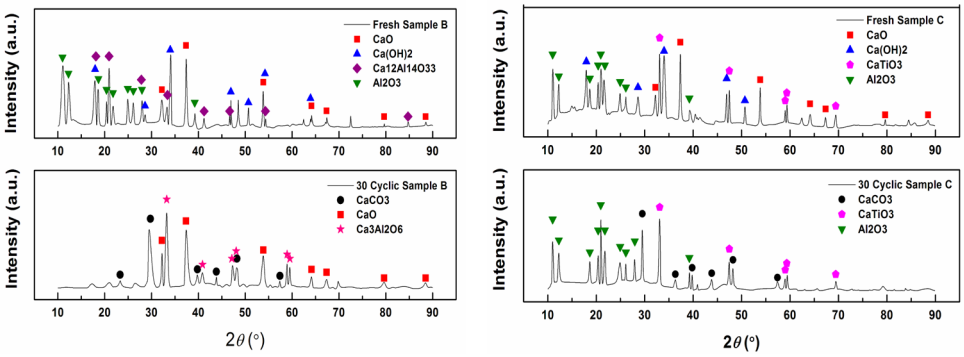

Figure 6. XRD patterns of the synthetic sample B and sample C before and after 30 calcination/calcination cycles under severe calcination condition of 900 °C in pure CO_2.

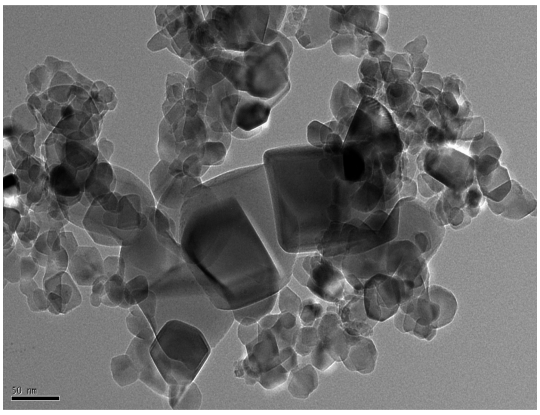

Figure 7. TEM images of TiO_2−Al_2O_3 skeleton (TiO_2−Al_2O_3 skeleton was derived from CaO/TiO_2−Al_2O_3 sorbent made by SATS method).

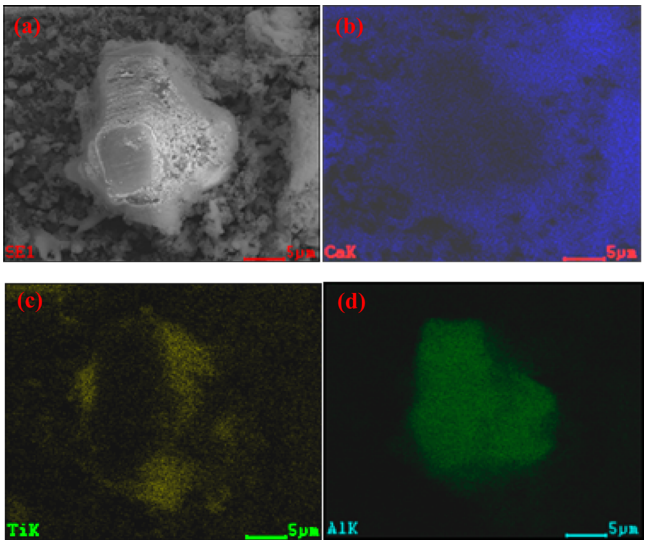

Figure 8. Energy dispersive spectrometer analysis of CaO/TiO_2−Al_2O_3 particle: (a) FSEM image, (b) Ca element map, (c) Ti element map, (d) Al element map.

glycerol,[54] demonstrated clearly that micron-level particles acted as core part and nanoparticles acted as shell part. Meanwhile, micron-level particles were decorated with a high coverage density of nanoparticle chains spreading outward from the micron-level particles to external boundary. In addition, the results of EDS test in Figure 8 provided sound proof of the core−shell structure: Al-based material acted as core part to undertake mechanical strength and sustained a stable frame to prevent sintering and agglomeration of novel sorbent, and Ti-based material was coated on Al_2O_3 to effectively inhibit the interaction between Ca-based active material and Al-based support. Thanks to this unique core−shell structure, SATS-derived CaO/TiO_2−Al_2O_3 sorbent performed higher CO_2 capture capacity and longer duration than CaO and CaO/Al_2O_3.

3.4. Crushing Strength of Three CaO-Based Sorbents.

A digital dynamometer was used to measure the force required to fracture a single particle sized between 0.2 and 0.3 mm, which represented crushing strength of fresh and used sorbents. The crushing strengths of fresh CaO, CaO/Al_2O_3, and CaO/TiO_2−Al_2O_3 were 1.46, 1.88, and 1.86 N respectively, compared with values of 1.08, 1.67, and 1.74 N for these samples after experiencing 30 cyclic tests (shown in SI Figure S12). It was considered that materials with crushing strength of above 1 N were suitable for large-scale industrial processes,[55] thus all three samples satisfied the strength demand in fluidized bed experiments. Further investigations on CO_2 capture performance of the novel sorbent in fluidized bed conditions are being conducted in our laboratory.

■ ASSOCIATED CONTENT

Supporting Information

Information about flame-synthesized nano-TiO_2, photos of preparation process, mass ration determination of CaO/TiO_2−Al_2O_3, processes of calculation formulas, curves of CO_2 capture capacity with reaction time in TG, evolution of carbonation conversion and carbonation reaction rate under mild and severe calcination condition, detailed analysis of pore size distribution, zeta potential of micron-Al_2O_3 and nano-TiO_2, and crushing strengths of sorbents. The Supporting Information is available free of charge on the ACS Publications website at DOI: 10.1021/acs.est.5b01415.

■ AUTHOR INFORMATION

Corresponding Author

*E-mail: klinsmannzhb@163.com, hzhao@mail.hust.edu.cn; phone: +86 27 8754 4779-8208; fax: +86 27 8754 5526.

Author Contributions

[§]Authors W.P. and Z.X. contributed equally. All authors have given approval to the final version of the manuscript.

DOI: 10.1021/acs.est.5b01415
Environ. Sci. Technol. 2015, 49, 8237−8245

Notes

The authors declare no competing financial interest.

■ ACKNOWLEDGMENTS

This work was funded by the National Natural Science Foundation of China (Grants 51390494 and 51276077). We are grateful to the Analytical and Testing Center of HUST for XRD, FSEM−EDS, and TEM measurements, and State Key Laboratory of Coal Combustion for BET−BJH tests.

■ REFERENCES

(1) Wong-Parodi, G.; Dowlatabadi, H.; McDaniels, T.; Ray, I. Influencing attitudes toward carbon capture and sequestration: A social marketing approach. *Environ. Sci. Technol.* **2011**, *45* (16), 6743−6751.

(2) Veltman, K.; Singh, B.; Hertwich, E. G. Human and environmental impact assessment of postcombustion CO_2 capture focusing on emissions from amine-based scrubbing solvents to air. *Environ. Sci. Technol.* **2010**, *44* (4), 1496−1502.

(3) Petrakopoulou, F.; Tsatsaronis, G.; Morosuk, T. Advanced exergoenvironmental analysis of a near-zero emission power plant with chemical looping combustion. *Environ. Sci. Technol.* **2012**, *46* (5), 3001−3007.

(4) Sathre, R.; Masanet, E. Long-term energy and climate implications of carbon capture and storage deployment strategies in the US coal-fired electricity fleet. *Environ. Sci. Technol.* **2012**, *46* (17), 9768−9776.

(5) Esposito, R. A.; Monroe, L. S.; Friedman, J. S. Deployment models for commercialized carbon capture and storage. *Environ. Sci. Technol.* **2010**, *45* (1), 139−146.

(6) Liu, W. Q.; Feng, B.; Wu, Y. Q.; Wang, G. X.; Barry, J.; da Costa, J. C. D. Synthesis of sintering-resistant sorbents for CO_2 capture. *Environ. Sci. Technol.* **2010**, *44* (8), 3093−3097.

(7) Florin, N. H.; Harris, A. T. Screening CaO-based sorbents for CO_2 capture in biomass gasifiers. *Energy Fuels* **2008**, *22* (4), 2734−2742.

(8) Li, Z.; Liu, Y.; Cai, N. Understanding the effect of inert support on the reactivity stabilization for synthetic calcium based sorbents. *Chem. Eng. Sci.* **2013**, *89*, 235−243.

(9) Feng, B.; An, H.; Tan, E. Screening of CO_2 adsorbing materials for zero emission power generation systems. *Energy Fuels* **2007**, *21* (2), 426−434.

(10) Donat, F.; Florin, N. H.; Anthony, E. J.; Fennell, P. S. Influence of high-temperature steam on the reactivity of CaO sorbent for CO_2 capture. *Environ. Sci. Technol.* **2012**, *46* (2), 1262−1269.

(11) Valverde, J. M.; Sanchez-Jimenez, P.; Perez-Maqueda, L. A. Relevant Influence of Limestone Crystallinity on CO_2 Capture in the Ca-Looping Technology at Realistic Calcination Conditions. *Environ. Sci. Technol.* **2014**, *48* (16), 9882−9889.

(12) Broda, M.; Manovic, V.; Anthony, E. J.; Müller, C. R. Effect of Pelletization and Addition of Steam on the Cyclic Performance of Carbon-Templated, CaO-Based CO_2 Sorbents. *Environ. Sci. Technol.* **2014**, *48* (9), 5322−5328.

(13) Broda, M.; Manovic, V.; Imtiaz, Q.; Kierzkowska, A. M.; Anthony, E. J.; Müller, C. R. High-Purity Hydrogen via the Sorption-Enhanced Steam Methane Reforming Reaction over a Synthetic CaO-Based Sorbent and a Ni Catalyst. *Environ. Sci. Technol.* **2013**, *47* (11), 6007−6014.

(14) Arias, B.; Grasa, G. S.; Alonso, M.; Abanades, J. C. Post-combustion calcium looping process with a highly stable sorbent activity by recarbonation. *Energy Environ. Sci.* **2012**, *5* (6), 7353−7359.

(15) Wang, J.; Anthony, E. J. On the decay behavior of the CO_2 absorption capacity of CaO-based sorbents. *Ind. Eng. Chem. Res.* **2005**, *44* (3), 627−629.

(16) Grasa, G. S.; Abanades, J. C. CO_2 capture capacity of CaO in long series of carbonation/calcination cycles. *Ind. Eng. Chem. Res.* **2006**, *45* (26), 8846−8851.

(17) Feng, B.; Liu, W.; Li, X.; An, H. Overcoming the Problem of Loss-in-Capacity of Calcium Oxide in CO_2 Capture. *Energy Fuels* **2006**, *20* (6), 2417−2420.

(18) Silaban, A.; Harrison, D. P. High Temperature Capture of Carbon Dioxide: Characteristics of the Reversible Reaction Between CaO(s) and CO_2(g). *Chem. Eng. Commun.* **1995**, *137* (1), 177−190.

(19) Li, Z.-s.; Fang, F.; Tang, X.-y.; Cai, N.-s. Effect of Temperature on the Carbonation Reaction of CaO with CO_2. *Energy Fuels* **2012**, *26* (4), 2473−2482.

(20) Abanades, J. C. The maximum capture efficiency of CO_2 using a carbonation/calcination cycle of CaO/$CaCO_3$. *Chem. Eng. J.* **2002**, *90* (3), 303−306.

(21) Manovic, V.; Anthony, E. J. Integration of Calcium and Chemical Looping Combustion using Composite CaO/CuO-Based Materials. *Environ. Sci. Technol.* **2011**, *45* (24), 10750−10756.

(22) Bhatia, S. K.; Perlmutter, D. D. Effect of the product layer on the kinetics of the CO_2-lime reaction. *AIChE J.* **1983**, *29* (1), 79−86.

(23) Li, Z.; Sun, H.; Cai, N. Rate Equation Theory for the Carbonation Reaction of CaO with CO_2. *Energy Fuels* **2012**, *26* (7), 4607−4616.

(24) Luo, C.; Shen, Q.; Ding, N.; Feng, Z.; Zheng, Y.; Zheng, C. Morphological Changes of Pure Micro- and Nano-Sized $CaCO_3$ during a Calcium Looping Cycle for CO_2 Capture. *Chem. Eng. Technol.* **2012**, *35* (3), 547−554.

(25) Liu, W.; An, H.; Qin, C.; Yin, J.; Wang, G.; Feng, B.; Xu, M. Performance enhancement of calcium oxide sorbents for cyclic CO_2 capture—A review. *Energy Fuels* **2012**, *26* (5), 2751−2767.

(26) Abanades, J. C.; Anthony, E. J.; Wang, J.; Oakey, J. E. Fluidized bed combustion systems integrating CO_2 capture with CaO. *Environ. Sci. Technol.* **2005**, *39* (8), 2861−2866.

(27) Valverde, J.; Perejón, A.; Perez-Maqueda, L. A. Enhancement of fast CO_2 capture by a nano-SiO_2/CaO composite at Ca-looping conditions. *Environ. Sci. Technol.* **2012**, *46* (11), 6401−6408.

(28) Luo, C.; Zheng, Y.; Ding, N.; Wu, Q.; Bian, G.; Zheng, C. Development and performance of CaO/La_2O_3 sorbents during calcium looping cycles for CO_2 capture. *Ind. Eng. Chem. Res.* **2010**, *49* (22), 11778−11784.

(29) Lu, H.; Khan, A.; Pratsinis, S. E.; Smirniotis, P. G. Flame-made durable doped-CaO nanosorbents for CO_2 capture. *Energy Fuels* **2008**, *23* (2), 1093−1100.

(30) Sun, R.; Li, Y.; Liu, H.; Wu, S.; Lu, C. CO_2 capture performance of calcium-based sorbent doped with manganese salts during calcium looping cycle. *Appl. Energy* **2012**, *89* (1), 368−373.

(31) Filitz, R.; Kierzkowska, A. M.; Broda, M.; Müller, C. R. Highly Efficient CO_2 Sorbents: Development of Synthetic, Calcium-Rich Dolomites. *Environ. Sci. Technol.* **2012**, *46* (1), 559−565.

(32) Broda, M.; Kierzkowska, A. M.; Müller, C. R. Influence of the Calcination and Carbonation Conditions on the CO_2 Uptake of Synthetic Ca-Based CO_2 Sorbents. *Environ. Sci. Technol.* **2012**, *46* (19), 10849−10856.

(33) Li, Y.; Sun, R.; Liu, H.; Lu, C. Cyclic CO_2 capture behavior of limestone modified with pyroligneous acid (PA) during calcium looping cycles. *Ind. Eng. Chem. Res.* **2011**, *50* (17), 10222−10228.

(34) Chen, H.; Zhao, C.; Yu, W. Calcium-based sorbent doped with attapulgite for CO_2 capture. *Appl. Energy* **2013**, *112*, 67−74.

(35) Manovic, V.; Anthony, E. J. CaO-based pellets supported by calcium aluminate cements for high-temperature CO_2 capture. *Environ. Sci. Technol.* **2009**, *43* (18), 7117−7122.

(36) Manovic, V.; Anthony, E. J. Lime-Based Sorbents for High-Temperature CO_2 Capture—A Review of Sorbent Modification Methods. *Int. J. Environ. Res. Public Health* **2010**, *7* (8), 3129−3140.

(37) Li, Y.; Su, M.; Xie, X.; Wu, S.; Liu, C. CO_2 capture performance of synthetic sorbent prepared from carbide slag and aluminum nitrate hydrate by combustion synthesis. *Appl. Energy* **2015**, *145*, 60−68.

(38) Chen, H.; Zhao, C.; Yang, Y.; Zhang, P. CO_2 capture and attrition performance of CaO pellets with aluminate cement under pressurized carbonation. *Appl. Energy* **2012**, *91* (1), 334−340.

DOI: 10.1021/acs.est.5b01415
Environ. Sci. Technol. 2015, 49, 8237−8245

(39) Manovic, V.; Anthony, E. J.; Grasa, G.; Abanades, J. C. CO_2 looping cycle performance of a high-purity limestone after thermal activation/doping. *Energy Fuels* **2008**, *22* (5), 3258−3264.
(40) Martavaltzi, C. S.; Lemonidou, A. A. Development of new CaO based sorbent materials for CO_2 removal at high temperature. *Microporous Mesoporous Mater.* **2008**, *110* (1), 119−127.
(41) Florin, N. H.; Blamey, J.; Fennell, P. S. Synthetic CaO-Based Sorbent for CO_2 Capture from Large-Point Sources. *Energy Fuels* **2010**, *24*, 4598−4604.
(42) Li, Z. S.; Cai, N. S.; Huang, Y. Y. Effect of preparation temperature on cyclic CO_2 capture and multiple carbonation-calcination cycles for a new Ca-based CO_2 sorbent. *Ind. Eng. Chem. Res.* **2006**, *45* (6), 1911−1917.
(43) Xu, Z.; Zhao, H. Simultaneous measurement of internal and external properties of nanoparticles in flame based on thermophoresis. *Combust. Flame* **2015**, *162* (5), 2200−2213.
(44) Arias, B.; Abanades, J.; Grasa, G. S. An analysis of the effect of carbonation conditions on CaO deactivation curves. *Chem. Eng. J.* **2011**, *167* (1), 255−261.
(45) Grasa, G.; González, B.; Alonso, M.; Abanades, J. C. Comparison of CaO-based synthetic CO_2 sorbents under realistic calcination conditions. *Energy Fuels* **2007**, *21* (6), 3560−3562.
(46) Manovic, V.; Anthony, E. J. Thermal activation of CaO-based sorbent and self-reactivation during CO_2 capture looping cycles. *Environ. Sci. Technol.* **2008**, *42* (11), 4170−4174.
(47) Manovic, V.; Anthony, E. J. Steam reactivation of spent CaO-based sorbent for multiple CO_2 capture cycles. *Environ. Sci. Technol.* **2007**, *41* (4), 1420−1425.
(48) Lu, H.; Khan, A.; Smirniotis, P. G. Relationship between structural properties and CO_2 capture performance of CaO-based sorbents obtained from different organometallic precursors. *Ind. Eng. Chem. Res.* **2008**, *47* (16), 6216−6220.
(49) Lu, H.; Smirniotis, P. G.; Ernst, F. O.; Pratsinis, S. E. Nanostructured Ca-based sorbents with high CO_2 uptake efficiency. *Chem. Eng. Sci.* **2009**, *64* (9), 1936−1943.
(50) Attard, P. Recent advances in the electric double layer in colloid science. *Curr. Opin. Colloid Interface Sci.* **2001**, *6* (4), 366−371.
(51) Ryde, N.; Kihira, H.; Matijević, E. Particle adhesion in model systems: 15. Effect of colloid stability in multilayer deposition. *J. Colloid Interface Sci.* **1992**, *151* (2), 421−432.
(52) Xu, Z.; Zhao, H.; Wei, Y.; Zheng, C. Self-assembly template combustion synthesis of a core-shell CuO@TiO_2-Al_2O_3 hierarchical structure as an oxygen carrier for the chemical-looping processes. *Combust. Flame* **2015**, *162*, 3030−3045 DOI: 10.1016/j.combustflame.2015.05.006.
(53) Wu, S. F.; Zhu, Y. Q. Behavior of $CaTiO_3$/Nano-CaO as a CO_2 Reactive Adsorbent. *Ind. Eng. Chem. Res.* **2010**, *49* (6), 2701−2706.
(54) Granados, M. L.; Alonso, D. M.; Sádaba, I.; Mariscal, R.; Ocón, P. Leaching and homogeneous contribution in liquid phase reaction catalysed by solids: The case of triglycerides methanolysis using CaO. *Appl. Catal., B: Environ.* **2009**, *89* (1−2), 265−272.
(55) Shulman, A.; Cleverstam, E.; Mattisson, T.; Lyngfel, A. Manganese/iron, manganese/nickel, and manganese/silicon oxides used in chemical-looping with oxygen uncoupling (CLOU) for combustion of methane. *Energy Fuels* **2009**, *23* (10), 5269−5275.

DOI: 10.1021/acs.est.5b01415
Environ. Sci. Technol. 2015, 49, 8237−8245